Application of Modern Control Algorithms to Improve Vehicle Suspension System Performance under Changing Dynamic Conditions

Reem Toumi
Tartous University
Tartous-al-Sawda

ABSTRACT
If the control system has fixed parameters, then designing a controller with fixed parameters is sufficient to improve its performance and response, However, in practical life, control systems are considered to have uncertain parameters, so designing controllers with fixed parameters does not meet the needs of control and regulation

Modern control algorithms that address the issue of regulation uncertain control systems include:

- Optimal parametric control, which has been highly successful in improving the performance of control systems with slowly changing parameters.
- Reference Model Adaptive Control (MRAC).

Vehicle suspension systems under changing dynamic conditions are considered a very important and complex system in practical life, involving uncertain parameters. Therefore, appropriate controllers must be designed to take these uncertainties into account. This paper studies the vehicle suspension system under changing dynamic conditions, controlling its time response, and taking into account the uncertainty of the control system parameters.

Keywords
Vehicle suspension system under changing dynamic conditions, optimal parametric controller, Adaptive control, Reference Model Adaptive Control (MRAC).

1. INTRODUCTION
The vehicle suspension system is considered one of the most important control systems in vehicles in general, especially buses that transport passengers for very long distances. This requires ensuring the comfort of passengers, especially since some passengers are sick, others are children or pregnant women. As a result of the use of public roads by fast vehicles of different weights, distortions may occur in the roads, which leads to the transportation vehicles being exposed to sudden disturbances that may frighten some passengers or may lead to harm to some passengers who sleep during the journey as a result of the sudden disturbance on the buses' wheels. Therefore, to reduce the impact of these disturbances, a suspension system is used that includes springs to mitigate the impact of disturbances resulting from road distortions or potholes that obstruct it. However, this system, represented by the suspension system, needs a controller so that it works to absorb disturbances in a smooth manner that does not affect the disturbance of the bus or vehicles in general, while taking into account the uncertainties of the control system. [1]

2. THE IMPORTANCE OF THE PAPER AND ITS OBJECTIVES
The importance of the paper is summarized in improving the performance and efficiency of the vehicle suspension system under changing dynamic conditions and with uncertainty of the control system parameters based on modern control algorithms that take the uncertainty of the control system into consideration, and knowing the uncertain parameters and their uncertainty ranges, as the control system includes the following components:

* Vehicle body with weight (m_1).
* The suspension system is a spring with a stiffness factor k_1 and a damping factor (b).
* Wheels of vehicle with weight m_2.
* A wheel frame which is equivalent to a spring with a stiffness factor of k_2.

The control system represented by the vehicle is a control system with two inputs, which are the control vector u(t) and the disturbance signal represented by the distortions and potholes in the road on which the vehicle is moving. The control system has two outputs, which are y_1, the displacement of the vehicle body, and y_2, the displacement of the vehicle wheels.

The paper also aims to develop a mathematical model of the vehicle's entire system, simulate it using Matlab/Simulink, and analyze the responses of the open-loop system. Practically, as the suspension system continues to operate, friction and damping factors change due to changes in temperature and humidity. The spring may lose its elasticity, thus reducing the efficiency of controllers designed for nominal values. Therefore, it is necessary to design robust controllers that take into account the uncertainty of the control system parameters and apply advanced control theories to design robust controllers.

3. REFERENCE STUDIES
Several advanced control algorithms have been used to control vehicle systems. The following papers studies have been used:

In paper [1], the suspension system, a critical component of a vehicle, was studied, playing a fundamental role in steering and comfort characteristics. This paper optimized the suspension system parameters to reduce vehicle vibrations. A magneto-rheological damper (MR damper) was added to a four-degree-of-freedom semi-car model. The effects of improving the suspension system's efficiency were studied, as well as the vehicle system modeled. The suspension system was simulated using MATLAB/Simulink, and the following algorithm was applied:

(PSO=The particle swarm optimization), To optimize the suspension parameters for vehicle vibration reduction and passenger comfort, the suspension parameters were optimized using two inputs:

link-bounded white noise and sine waves. The results showed that adding a magneto-rheological damper in any mode reduced vehicle vibration. The maximum reduction in vehicle vibration was associated with the condition in which all suspension parameters were optimized, and the objective function value in that case was improved by about 32%.

In paper [2], electric vehicles (EVs) were studied, which are considered alternative vehicles in the automotive industry, providing lower exhaust emissions. This paper developed an internal-drive switched reluctance motor (SRM) propulsion system for an electric vehicle. SRM propulsion systems are cheaper and do not use complex components, unlike permanent magnet motors (PMMs). However, the internal-drive SRM system suffers from a disadvantage, which is the increased mass of the suspension system when compared to a PMM propulsion system that provides the same equivalent power. This situation leads to an increase in the mass of the wheels, and therefore a suspension analysis is required. This paper discussed the suspension dynamics evaluated using a simulation of an internal-drive SRM electric vehicle, and compared it to an internal-combustion engine (ICE) vehicle. The simulation used design scenarios derived from graded loads, namely (1) the driver's seat with springs, (2) the driver's seat without springs. Bode diagram analysis techniques were also used to determine the ride comfort range of the developed electric vehicle.

In paper [3], the vehicle's shock absorbers were designed by identifying the optimal point based on our needs. The system was analyzed for any disturbances, and then the entire vehicle was modeled as a two-degree-of-freedom system, and a modular analysis was performed. The frequency ratio (r) was carefully chosen. The displacement transmission can be reduced with a large (r), but at the same time, the force transmission increases at a large (r). This situation is very disturbing for the passenger, who will feel the sudden impact. Suspension design is not limited to simply reducing mass vibration. Of course, if the wheels begin to separate from the ground, the vehicle's handling will become poor, as an overly soft suspension system suffers from poor control. Therefore, designers must choose between control and vibration isolation. Similarly, an attempt was made to maintain the response of the front and rear wheels as similar as possible to ensure smooth driving. This is evident from the response of the control system obtained in the typical analysis. Two vibration modes can be observed: In the first case, the translational motion is more dominant and tends more toward a regular sinusoid, while in the second case, the slope motion plays a greater role, distorting the response and producing different peaks at different times. The accuracy of the analysis can be further increased by modeling the system with higher degrees of freedom. A multi-degree-of-freedom system can be solved by calculating the translation function and providing the rule inputs using SIMULINK, which can yield better and more accurate results.

4. MATHEMATICAL MODELING OF VEHICLE SUSPENSION SYSTEMS [1][2][3][4][5][6]

This section will present a dynamic mathematical model of the vehicle suspension system, where the kinematic and dynamic equations will be found, taking into account the uncertainty of the suspension system parameters. Figure (1) shows a description of the vehicle suspension system studied in this paper:

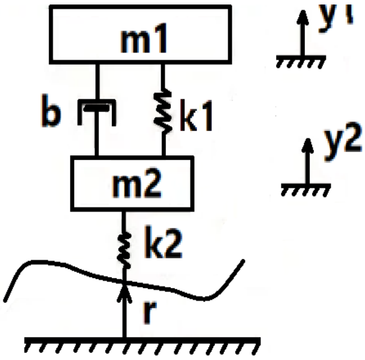

Figure 1" Structural diagram of vehicle suspension system

Whereas:

m_1 Vehicle body weight.

m_2 Vehicle wheel weight.

k_1 Spring stiffness factor that represents the suspension system.

k_2 Spring stiffness factor equivalent to wheel rim.

b Suspension damping factor.

y_1 Vehicle body displacement.

y_2 Wheel displacement.

r The displacement of the frames relative to the ground represents the noise signal.

At this stage, the dynamic equations of a vehicle suspension system will be derived using one of two methods:

The first method: applying the Newton-Euler method.

The second method: applying the Lagrange principle.

This paper will use the Lagrange principle.

The general dynamical Lagrange equation for non-holonomic WMR systems is given by the following equation (1):

$$\frac{d}{dt}\left(\frac{\partial L}{\partial \dot{\boldsymbol{q}}}\right) - \frac{\partial L}{\partial \boldsymbol{q}} + \boldsymbol{M}^T(q)\boldsymbol{\lambda} = \boldsymbol{E}(q)\boldsymbol{\tau} \quad (1)$$

Where: L is the Lagrange function and is defined as the difference between the kinetic energy of the body K and its potential energy P:

$$L = K - P \quad (2)$$

Whereas:

$\boldsymbol{q}$ Motion vector.

$\boldsymbol{\tau}$ Input vector.

$\boldsymbol{D}(\boldsymbol{q})$ System inertia matrix.

$\boldsymbol{E}(\boldsymbol{q})$ Input matrix.

$\boldsymbol{M}(\boldsymbol{q})$ Matrix in motion.

$\boldsymbol{\lambda}$ Vector Lagrange factorials.

From equation (1), we obtain the dynamic equation for a system subject to a kinetic constraint in the following form, neglecting the limits of the gravitational forces $\boldsymbol{G(q)}$ and the Coriolis forces $\boldsymbol{V(q,\dot{q})}$, considering that the suspension system moves in the XY plane at low speeds:

$$\boldsymbol{D}(q)\ddot{\boldsymbol{q}} + \boldsymbol{M}^T(q)\boldsymbol{\lambda} = \boldsymbol{E}(q)\boldsymbol{\tau} \tag{3}$$

Based on Figure (2) which shows the suspension system with the control vector u(t):

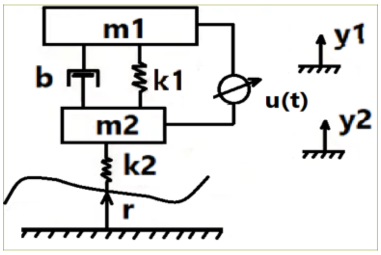

Figure 2 Suspension system with control vector u(t)

Then, by applying Lagrange's principle, we obtain the dynamic equations of the vehicle suspension system according to the following formulas (4) and (5):

$$\ddot{y}_1 + \frac{k_1}{m_1}(y_1 - y_2) + \frac{b}{m_1}(\dot{y}_1 - \dot{y}_2) = \frac{1}{m_1}u(t) \tag{4}$$

$$\ddot{y}_2 - \frac{k_1}{m_2}(y_1 - y_2) - \frac{b}{m_2}(\dot{y}_1 - \dot{y}_2) + \frac{k_2}{m_2}(y_2 - r) = -\frac{1}{m_2}u(t) \tag{5}$$

4.1 Representation of Vehicle Suspension System in State Space

According to equations (4) and (5), we assume:

$$x_1(t) = y_1(t) \quad , \quad x_2(t) = \dot{y}_1(t)$$
$$x_3(t) = y_2(t) \quad , \quad x_4(t) = \dot{y}_2(t) \tag{6}$$

By deriving hypotheses (6), we find:

$$\dot{x}_1(t) = \dot{y}_1(t) \quad , \quad \dot{x}_2(t) = \ddot{y}_1(t)$$
$$\dot{x}_3(t) = \dot{y}_2(t) \quad , \quad \dot{x}_4(t) = \ddot{y}_2(t) \tag{7}$$

Using equations (4), (5) and (6) we obtain the equations of state representing the open-loop vehicle suspension system:

$$\dot{x}_1(t) = x_2(t)$$

$$\dot{x}_2(t) = -\frac{k_1}{m_1}(x_1(t) - x_3(t)) - \frac{b}{m_1}(x_2(t) - x_4(t)) + \frac{1}{m_1}u(t) \tag{8}$$

$$\dot{x}_3(t) = x_4(t)$$

$$\dot{x}_4(t) = \frac{k_1}{m_2}(x_1(t) - x_3(t)) + \frac{b}{m_2}(x_2(t) - x_4(t)) - \frac{k_2}{m_2}(x_3(t) - r(t)) - \frac{1}{m_2}u(t)$$

$$y_1(t) = x_1(t)$$

$$y_2(t) = x_3(t)$$

From equation (8) we obtain the radial formula for the vehicle suspension system:

$$\begin{bmatrix}\dot{x}_1(t)\\ \dot{x}_2(t)\\ \dot{x}_3(t)\\ \dot{x}_4(t)\end{bmatrix} = \begin{bmatrix} 0 & 1 & 0 & 0 \\ -\frac{k_1}{m_1} & -\frac{b}{m_1} & \frac{k_1}{m_1} & \frac{b}{m_1} \\ 0 & 0 & 0 & 1 \\ \frac{k_1}{m_2} & \frac{b}{m_2} & -\frac{k_1}{m_2} - \frac{k_2}{m_2} & -\frac{b}{m_2} \end{bmatrix} \begin{bmatrix} x_1(t)\\ x_2(t)\\ x_3(t)\\ x_4(t)\end{bmatrix} + \begin{bmatrix} 0 \\ \frac{1}{m_1} \\ 0 \\ -\frac{1}{m_2}\end{bmatrix} u(t) + \begin{bmatrix} 0\\ 0\\ 0\\ \frac{k_2}{m_2}\end{bmatrix} r(t) \tag{9}$$

$$\begin{bmatrix} y_1(t)\\ y_2(t)\end{bmatrix} = \begin{bmatrix} 1 & 0 & 0 & 0 \\ 0 & 0 & 1 & 0\end{bmatrix} \begin{bmatrix} x_1(t)\\ x_2(t)\\ x_3(t)\\ x_4(t)\end{bmatrix} + \begin{bmatrix}0\\0\end{bmatrix} u(t) + \begin{bmatrix}0\\0\end{bmatrix} r(t)$$

4.2 Vehicle Suspension System Simulation using Matlab/Simulink:[3][4][5][6][7][8][9]

By simulating the vehicle suspension system represented by equations (4) and (5) using the Matlab/Simulink program, we obtain the diagram of the open-loop control system shown in Figure (3):

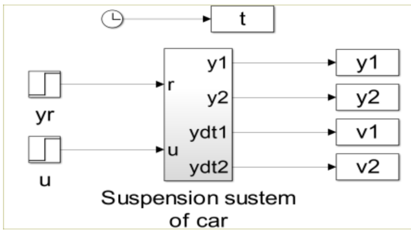

Figure 3 Open loop vehicle suspension system

Figure (4) also shows the detailed diagram of the vehicle suspension system shown in Figure (3):

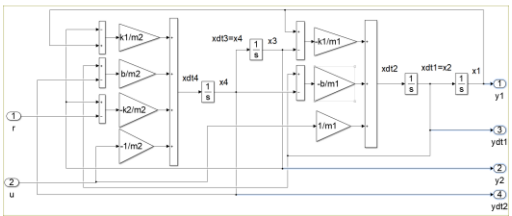

Figure 4 Detailed diagram of the open-loop vehicle suspension system

4.3 Suspension responses in open-loop vehicles:[7][8][9][10][11][12]

Table (1) shows the vehicle suspension system parameters used in the simulation:

Table 1 Vehicle suspension system parameters

The symbol	Description	value
m_1	Vehicle body weight	$300\ (kg)$
m_2	Vehicle wheel weight	$60\ (kg)$
k_1	Spring stiffness factor that represents the suspension system	$16000\ (N/m)$
k_2	Spring stiffness factor equivalent to a wheel frame	$190000\ (N/m)$
b	Suspension damping factor	$1000\ (N/m.sec)$

In the simulation, we will assume that the vehicle is traveling on a completely flat road with no distortions, and thus the noise signal $r(t) = 0$. By implementing the simulation scheme shown in Figure (3), we obtain the following responses:

- **Open loop response to vehicle body displacement y_1:**

Figure (5) shows the open-loop response to the vehicle body displacement $y_1(t)$:

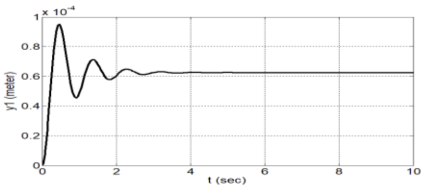

Figure 5 Open loop response to vehicle body displacement $y_1(t)$

- **Open loop response to wheel displacement:**

Figure (6) shows the open-loop response to the displacement of the cart wheels $y_2(t)$:

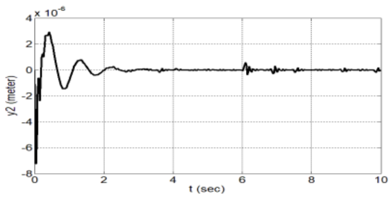

Figure 6 The open-loop response to the displacement of the cart wheels $y_2(t)$

- **Open loop response to vehicle body displacement velocity:**

Figure (7) shows the open-loop response to the vehicle body displacement velocity:

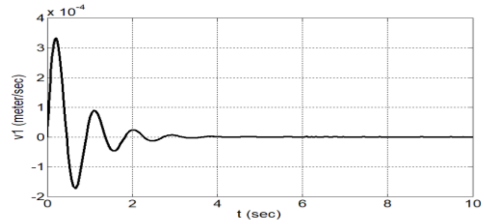

Figure 7 Open loop response to vehicle body displacement velocity

- **Open loop response to vehicle wheel displacement velocity:**

Figure (8) shows the open-loop response to the vehicle wheel displacement velocity:

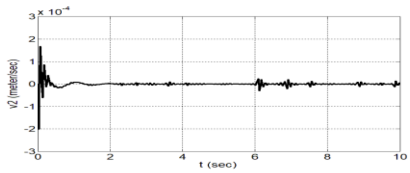

Figure 8 Open loop response to vehicle wheel displacement velocity

From the previous responses, especially the vehicle displacement response $y_1(t)$, the response is very bad and leads to a very large displacement estimated at $60\ cm$, which is a displacement that leads to major vehicle accidents. When there are distortions in the road, the displacement will get worse, so it is necessary to design appropriate controllers to reduce these displacements.

5. OPTIMAL PARAMETRIC CONTROLLER DESIGN [13][14][15]

We will first learn how to design a linear quadratic optimal controller based on state variables.

5.1 Quadratic linear optimal controller:

The optimal controller relies on generating a control vector based on state variables, giving us a wide range of control over the dynamics of the control system. The mathematical model of the control system based on state variables is given by the following formula:

$$\dot{x} = Ax + Bu \qquad y = Cx \tag{10}$$

The diagram plot represented in Figure (9) represents the equations of the previous case:

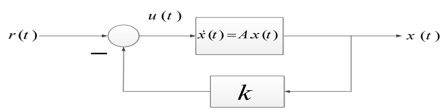

Figure 9 Block diagram of the optimal control problem

The quadratic linear optimal control vector is given by the following relation:

$$u_{opt} = \mathrm{r(t)} - k_{optimal}x(t) \tag{11}$$

Then the block diagram of the control set with the optimal controller becomes as shown in Figure (10):

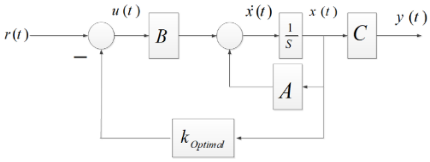

Figure 10 Detailed diagram of the optimal control problem based on state equations

The optimal control gain is given by the following formula:

$k_{optimal} = R^{-1}B^TP$	(12)

Where P is a positively defined symmetric matrix and is a solution to the following Riccati differential equation:

$$PA + A^TP - PBR^{-1}BP + Q = 0 \quad (13)$$

The performance function to be minimized has the following formula:

$J = \frac{1}{2}\int_0^{t_f}(x^TQx + Ru^2)dt$	(14)

5.2 Representation of the suspicious control plant in the form of a direct connection with $\boldsymbol{\delta}$:

The linear quadratic optimal controller offers significant advantages when designed for a nominal control system, but it can lose its robustness and performance when the control system parameters become uncertain. Therefore, the optimal controller design approach had to be modified. Before designing the optimal parametric controller, the control system must be formulated using the direct correlation formula with δ. According to this formula, the uncertain parameter is represented by a coefficient δ, as in the following formula:

$P_1 = \frac{P_1 + \bar{P}_1}{2} + \frac{\bar{P}_1 - P_1}{2}\delta_1$ $P_2 = \frac{P_2 + \bar{P}_2}{2} + \frac{\bar{P}_2 - P_2}{2}\delta_2$	(15)

Whereas: $\delta_i \in [-1, +1]$

f the control plant has the following form:

$\dot{x} = \tilde{A}x + Bu$	(16)

Then the control plant can be written in direct relation form with $\boldsymbol{\delta}$ as follows:

$\dot{x} = (A_0 + \sum_{i=1}^{l} A_i\delta_i)x(t) + Bu(t)$	(17)

5.3 Optimal parametric controller design:[14][15][16][17]

Theory:

A model of state equations represented by the direct coupling form with $\boldsymbol{\delta}$ is Lyapunov stable if there is a positively defined matrix (L_C) that satisfies the following Lyapunov inequality:

$L_CA(\Delta^{(k)}) + A^T(\Delta^{(K)})L_C < -\xi \quad : \quad k = 1,2,\ldots$	(18)

This is for the heads of the entire space, which is defined by the suspicious parameters. If we have three parameters that form the space shown in Figure (11):

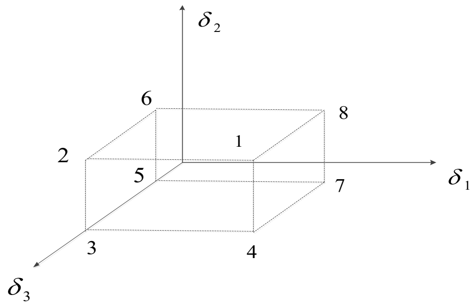

Figure 11 The space vertices specified for three suspicious parameters.

There must exist (L_C) that satisfies the Lyapunov inequalities given in equations (*19*):

$L_CA(\Delta^{(1)}) + A^T(\Delta^{(1)})L_C < -\xi$ $L_CA(\Delta^{(2)}) + A^T(\Delta^{(2)})L_C < -\xi$ ….. $L_CA(\Delta^{(8)}) + A^T(\Delta^{(8)})L_C < -\xi$	(19)

Whereas:

$A(\Delta^{(1)})$ is the matrix $(\tilde{A})$ at vertex (1) that represents the values of the parameters:

$\delta_1 = \bar{\delta}_1, \delta_2 = \bar{\delta}_2, \delta_3 = \bar{\delta}_3$	(20)

$A(\Delta^{(8)})$ is the matrix $(\tilde{A})$at vertex (8).

To design the optimal parametric controller, we write the direct correlation formula for $\boldsymbol{\delta}$ as follows:

$\dot{x} = (A_0 + \sum_{j=1}^{l} A_j\delta_j)x + Bu$ $\dot{x} = (A_0 + L_1N_1^T\delta_1 + L_2N_2^T\delta_2 + \ldots\ldots)x + Bu$	(21)

Where L_1, L_2, N_1, N_2 are perpendicular rays of dimensions $(n \times 1)$ so that they are chosen to achieve:

$A_1 = L_1N_1^T, A_2 = L_2N_2^T, \ldots$	(22)

Then we form the two augmented matrices as follows:

$L = [L_1 \quad L_2 \quad L_3 \ldots.]$ $N = [N_1 \quad N_2 \quad N_3 \ldots.]$	(23)

Then we replace the previous Riccati equation with the following modified Riccati algebraic equation:

$A_0^TS + SA_0 - S[\frac{1}{\rho}BB^T - \frac{1}{\gamma}LL^T]S + Q_0 + \gamma NN^T = 0$	(24)

Where γ, ρ are design parameters, if we assume that:

$B_0 = \frac{1}{\rho}BB^T - \frac{1}{\gamma}LL^T$ $C_0 = Q_0 + \gamma NN^T$	(25)

The Riccati algebraic equation becomes:

$A_0^TS + SA_0 - SB_0S + C_0 = 0$	(26)

This equation is similar to Riccati's algebraic equation:

$$A^T P + PA - PBP + C = 0 \qquad (27)$$

Which can be solved using MATLAB using the instruction:

$$>> P = are(A, B, C) \qquad (28)$$

That *is:*

$$>> S = are(A_0, B_0, C_0) \qquad (29)$$

Then the optimal parametric control vector is given by the optimal parametric regulator method in the formula:

$$u = -Gx \qquad (30)$$

where (G) is the gain vector:

$$G = \frac{1}{\rho} R^{-1} B^T S \qquad (31)$$

In this case, the solution is done under the presence of the two constraints (γ, ρ), and the solution conditions are the presence of (S) defined positively. If the assumed values of (γ, ρ) are not suitable, they can be changed and the appropriate (S) can be found.

5.4 Representing the suspension system in direct correlation form with $\boldsymbol{\delta}$

We will assume that the parameters k_1 , k_2 , and b are uncertain by $\pm 20\%$ of their nominal values, according to Table (2):

Table (2) Uncertainty range of suspension system parameters used in vehicles

The symbol	nominal value	Max value	Min value
k_1	16000 $(^N/_m)$	*19200* $(^N/_m)$	*12800* $(^N/_m)$
k_2	190000 $(^N/_m)$	*228000* $(^N/_m)$	*152000* $(^N/_m)$
b	1000 $(^N/_{m.se}$	*1200* $(^N/_{m.sec})$	*800* $(^N/_{m.sec})$

$$\begin{bmatrix}\dot{x}_1(t)\\ \dot{x}_2(t)\\ \dot{x}_3(t)\\ \dot{x}_4(t)\end{bmatrix} = \left\{\begin{bmatrix} 0 & 1 & 0 & 0\\ -58.6667 & -3.6667 & 58.6667 & 3.6667\\ 0 & 0 & 0 & 1\\ 293.3333 & 18.3333 & -3776.7 & -18.3333\end{bmatrix} + \begin{bmatrix} 0 & 0 & 0.0000 & 0\\ -5.3333 & 0 & 5.33330 & 0\\ 0 & 0 & 0 & 0\\ 26.6667 & 0 & -26.6667 & 0\end{bmatrix}\delta_1 + \begin{bmatrix} 0 & 0 & 0.0000 & 0.0000\\ 0 & 0 & 0.00000 & 0.0000\\ 0 & 0 & 0.0000 & 0.0000\\ 0 & 0 & -316.6667 & 0\end{bmatrix}\delta_2 + \begin{bmatrix} 0 & 0.0000 & 0.0000 & 0.000\\ 0 & -0.3333 & 0.0000 & 0.3333\\ 0 & 0 & 0 & 0\\ 0 & 1.6667 & 0 & -1.6667\end{bmatrix}\delta_3\right\}\begin{bmatrix}x_1(t)\\ x_2(t)\\ x_3(t)\\ x_4(t)\end{bmatrix} + \begin{bmatrix}0\\ 0.0033\\ 0\\ -0.0167\end{bmatrix}u(t) + \begin{bmatrix}0\\ 0\\ 0\\ 3166.7\end{bmatrix}r(t) \qquad (34)$$

Hence we assume:

Following the steps of representing the control plant in the form of a direct connection with δ, we find:

$$k_1 = \frac{\underline{k}_1 + \bar{k}_1}{2} + \frac{\bar{k}_1 - \underline{k}_1}{2}\delta_1 = 17600 + 1600\delta_1$$
$$k_2 = \frac{\underline{k}_2 + \bar{k}_2}{2} + \frac{\bar{k}_2 - \underline{k}_2}{2}\delta_2 = 209000 + 19000\delta_2$$
$$b = \frac{\underline{b}_1 + \bar{b}_1}{2} + \frac{\bar{b}_1 - \underline{b}_1}{2}\delta_3 = 1100 + 100\delta_3 \qquad (32)$$

We substitute in the state equations (9) and find:

$$\begin{bmatrix}\dot{x}_1(t)\\ \dot{x}_2(t)\\ \dot{x}_3(t)\\ \dot{x}_4(t)\end{bmatrix} = \begin{bmatrix} 0 & 1\\ -58.6667 - 5.3333\delta_1 & -3.6667 - 0.3333\delta_3\\ 0 & 0\\ 293.3333 + 26.6667\delta_1 & 18.3333 + 1.6667\delta_3\end{bmatrix} + \begin{bmatrix}0\\ 0.0033\\ 0\\ -0.0167\end{bmatrix}u(t) + \begin{bmatrix}0\\ 0\\ 0\\ 3166.7\end{bmatrix}r(t) \qquad (33)$$

$$\begin{bmatrix}y_1(t)\\ y_2(t)\end{bmatrix} = \begin{bmatrix}1 & 0 & 0 & 0\\ 0 & 0 & 1 & 0\end{bmatrix}\begin{bmatrix}x_1(t)\\ x_2(t)\\ x_3(t)\\ x_4(t)\end{bmatrix} + \begin{bmatrix}0\\ 0\end{bmatrix}u(t) + \begin{bmatrix}0\\ 0\end{bmatrix}r(t)$$

Hence, we find the state equations according to the direct correlation formula with δ:

$$A_0 = \begin{bmatrix} 0 & 1 & 0 & 0\\ -58.6667 & -3.6667 & 58.6667 & 3.6667\\ 0 & 0 & 0 & 1\\ 293.3333 & 18.3333 & -3776.7 & -18.333\end{bmatrix} \qquad (35)$$

$$A_1 = \begin{bmatrix} 0 & 0 & 0.0000 & 0\\ -5.3333 & 0 & 5.33330 & 0\\ 0 & 0 & 0 & 0\\ 26.6667 & 0 & -26.6667 & 0\end{bmatrix} = L_1 N_1^T$$

$$A_2 = \begin{bmatrix} 0 & 0 & 0.0000 & 0.0000\\ 0 & 0 & 0.00000 & 0.0000\\ 0 & 0 & 0.0000 & 0.0000\\ 0 & 0 & -316.6667 & 0\end{bmatrix} = L_2 N_2^T$$

$$A_3 = \begin{bmatrix} 0 & 0.0000 & 0.0000 & 0.000\\ 0 & -0.3333 & 0.0000 & 0.3333\\ 0 & 0 & 0 & 0\\ 0 & 1.6667 & 0 & -1.6667\end{bmatrix} = L_3 N_3^T$$

From it we find:

$$L_1^T = [0 \quad 2.3094 \quad 0 \quad -11.547]$$
$$N_1^T = [-2.3094 \quad 0 \quad 2.3094 \quad 0] \qquad (36)$$

$$L_2^T = [0 \quad 0 \quad 0 \quad -17.7951]$$
$$N_2^T = [0 \quad 0 \quad 17.7851 \quad 0]$$
$$L_3^T = [0 \quad 0.5773 \quad 0 \quad -2.8871]$$
$$N_3^T = [0 \quad -0.5773 \quad 0 \quad 0.5773]$$

From equations (36) we obtain the following two uncertainty matrices:

$$L = \begin{bmatrix} 0 & 0 & 0 \\ 2.3094 & 0 & 0.5773 \\ 0 & 0 & 0 \\ -11.547 & -17.7951 & -2.8871 \end{bmatrix} \qquad (37)$$
$$N = \begin{bmatrix} -2.3094 & 0 & 0 \\ 0 & 0 & -0.5773 \\ 2.3094 & 17.7851 & 0 \\ 0 & 0 & 0.5773 \end{bmatrix}$$

5.5 Vehicle suspension system responses when using the optimal parametric controller

By applying the optimal parametric control methodology described in paragraph (5-3) and for the uncertainty shown in Table (2), we obtain the following simulation results:

5.5.1 Optimal Parametric Controller Design Results for Nominal Parameters

For the nominal values of the suspension parameters in vehicles we obtain the following responses:

- **Response to vehicle body displacement y_1:**

Figure (12) shows the response to the vehicle body displacement $y_1(t)$ when using the optimal parametric controller:

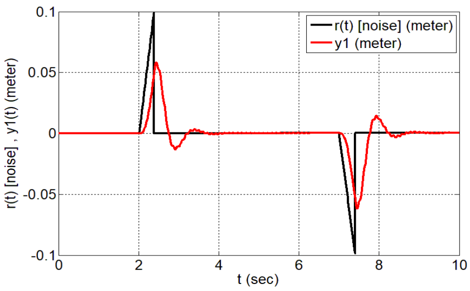

Figure 12 Response to vehicle body displacement $y_1(t)$ when using the optimal parametric controller at the nominal values of the parameters

- **Response to displacement of the cart wheels y_2:**

Figure (13) shows the response to the displacement of the cart wheels y_2 when using the optimal parametric controller:

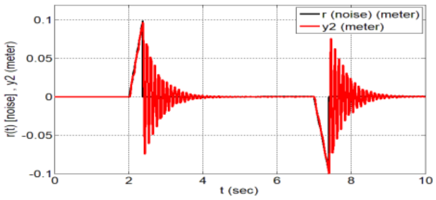

Figure 13 Response to vehicle wheel displacement $y_2(t)$ when using the optimal parametric controller at the nominal values of the parameters

5.5.2 Optimal Parametric Controller Design Results from Parameter Uncertainty

In order to determine the parameters of the suspension system in vehicles according to Table (2), we obtain the following responses:

- **Response to vehicle body displacement y_1:**

Figure (14) shows the response to the displacement of the vehicle body $y_1(t)$ when using the optimal parametric controller for the maximum and minimum uncertainty of the parameters:

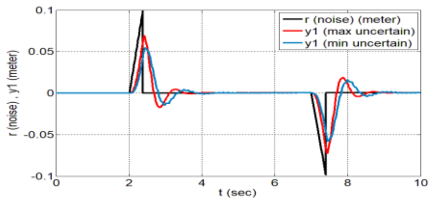

Figure 14 Response to vehicle body displacement $y_1(t)$ when using the optimal parametric controller for maximum and minimum uncertainty in the parameters

- **Response to displacement of the cart wheels y_2:**

Figure (15) shows the response to the vehicle wheel displacement $y_2(t)$ when using the optimal parametric controller for maximum and minimum uncertainty in the parameters:

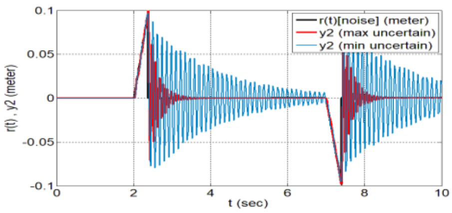

Figure 14 Response to vehicle wheel displacement $y_2(t)$ when using the optimal parametric controller for maximum and minimum uncertainty in the parameters

Through the previous responses, especially the vehicle displacement response $y_1(t)$ shown in Figure (12) and corresponding to the nominal values of the parameters, we note that the response is very good, as the maximum displacement of the vehicle body reached about (0.05 meters) for the maximum road deformation (0.1 meters) and the minimum (-0.1 meters). We note that within a time of less than (1 sec) the level of the vehicle returned to a completely straight position. When the vehicle total parameters are uncertain due to the decline in the flexibility of the suspension system due to the temperature and surrounding climatic conditions, and according to Figure (14), we note that for the maximum uncertainty the displacement of the vehicle body reached (0.06 meters), and at the minimum uncertainty the displacement of the vehicle body reached (0.05 meters). Thus, we conclude the success of the parametric controller in absorbing the maximum and minimum road deformations, which leads to good passenger comfort. The optimal parametric controller also succeeded in maintaining its strong performance when the suspension total parameters are uncertain. The vehicle's displacement is significantly greater than $\pm 20\%$. According to Figures (13) and (15), which show the vehicle's wheel displacement response $y_2(t)$, we note that the maximum displacement is 0.1 meters for the nominal values of the parameters and the maximum and minimum uncertainty in the parameters. It is worth noting that the vehicle's body response is most important because it contains passengers whose calm and comfort are to be maintained during travel, even when exposed to various road deformations.

6. DESIGN OF THE MRAC REFERENCE MODEL ADAPTIVE CONTROLLER [18][19][20][21][22][23]

6.1 General block diagram of MRAC adaptive controller

The MRAC technique was introduced in 1958 by Whitacker, and the general block diagram of this method is shown in Figure (16) below:

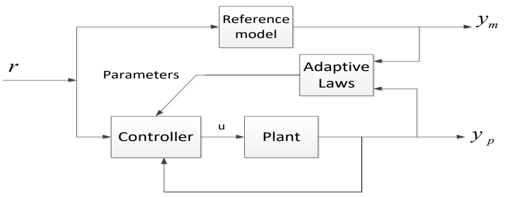

Figure 16 The basic structure of the MRAC reference model adaptive control system

The primary regulator y_p is used to achieve the appropriate closed-loop behavior. This is a non-adaptive loop. Because the control parameters are unknown or time-varying, a regulator with fixed parameters cannot be designed. Therefore, in the MRAC technique, the reference model is used, as its response is the desired response. The adaptation mechanism must track the control output signal to the reference model output signal y_m. The adaptation mechanism continues to operate until the error between the two outputs becomes zero. Also, the state variables of the control system $x_p$can track the state variables of the reference model x_m. The most important advantage of the MRAC scheme is that it achieves direct adaptation to the uncertainty of the control parameters without the need to estimate the parameters.

According to the diagram shown in Figure (16), the MRAC adaptive control system consists of two feedback loops:

The first loop: an internal feedback loop consisting of the primary regulator.

The second loop: an external feedback loop consisting of the adaptive mechanism.

Typically, the inner loop operates faster than the second loop because the statement parameters change at a slower rate compared to the change in the control statement states. According to Figure (16), the reference model is linked to the branching of the control plant.

6-1 Steps for designing a reference model adaptive controller (MRAC):

A M.R.A.C system consists of the following basic components:

- Control system.
- Basic controller.
- Reference model.
- Deriving adaptive laws.

The reference model defines the desired behavior of the control system and is usually parameterized so that it can be implemented on a computer. If the study relies on the state variables of the control system, the reference model is given as a complete state vector. The reference model must meet certain requirements: its relative degree is equal to the relative degree of the control system. Furthermore, it must be stable, fully controllable, sensitive, and responsive. The key to designing a M.R.A.C system is deriving adaptive laws. The adaptive controller with the reference model will be designed based on the state equations.

6.2 Steps for designing a reference model adaptive controller (MRAC):

If the control system is linear, of order n, fully controllable, and has no zeros, then the control vector that displaces the closed-loop poles has the following form:

$$u = k_b x_p + k_0 r \quad (38)$$

If the open control plant is described by the following transfer function:

$$W_p(s) = \frac{b_{pn}}{s^n + a_{pn}s^{n-1} + a_{p(n-1)}s^{n-2} + \dots + a_{p2}s^1 + a_{p1}} \quad (39)$$

Then this plant can be described by the equations of state according to the controllability formula as follows:

$$\dot{x}_p = A_p x_p + B_p u$$
$$y_p = C^T x_p \quad (40)$$

The control plant is written according to the controllability formula, where the control plant is represented in the form (17) where u(t) is the control vector:

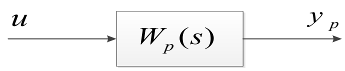

Figure 17 Open loop control plant

By closing the open system with negative feedback using the following control vector:

$$u = k_b x_p + k_0 r \quad (41)$$

Whereas:

$$k_b = [k_1 \quad k_2 \quad \dots \quad k_n]_{1\times n}, x_p = [x_1 \quad x_2 \quad \dots \quad x_n]^T_{n\times 1}$$
$$k_0(1\times 1), r(1\times 1) \quad (42)$$

By representing the control vector, the closed control plant becomes represented in Figure (18):

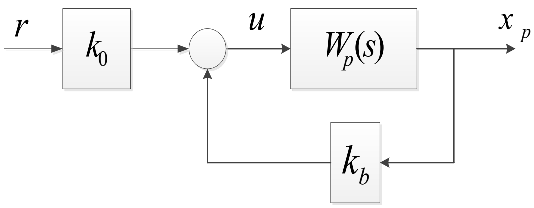

Figure 18 Closed loop control system.

The control ray can be written in the following form:

$$u = \theta^T . \omega \tag{43}$$

Whereas:

$$\theta^T = \begin{bmatrix} k_0 & k_b \end{bmatrix}, \ \omega^T = \begin{bmatrix} r & x_p \end{bmatrix}^T \tag{44}$$

Hence, the state equations for the closed system after changing the control vector in the state equations become as follows:

$$\begin{aligned} \dot{x}_p &= A_p x_p + B_p (k_b x_p + k_0 r) \\ y_p &= C^T x_p \end{aligned} \tag{45}$$

From it we find:

$$\begin{aligned} \dot{x}_p &= (A_p + B_p k_b) x_p + B_p k_0 r \\ y_p &= C^T x_p \end{aligned} \tag{46}$$

And from it the equations of state for a closed system:

$$u = k_b x_p + k_0 r \tag{47}$$

Whereas:

$$\begin{aligned} A_c &= A_p + B_p k_b \ , B_c = B_p k_0 \\ C^T &= C_c^T \end{aligned} \tag{48}$$

Since the control system parameters $a_{pn}, a_{p(n-1)}, \ldots, a_{p2}, a_{p1}, b_{pn}$ are constant but unknown, the regulator parameters k_b, k_0 are adjusted using an adaptive mechanism. The adjustment mechanism is generated by tracking the control system output signal to the output signal of a reference model chosen to achieve an optimal response. If the reference model is given by the following transfer function:

$$W_m(s) = \frac{b_{mn}}{s^n + a_{mn} s^{n-1} + a_{m(n-1)} s^{n-2} + \ldots + a_{m2} s^1 + a_{m1}} \tag{49}$$

The equations of state for the reference model are:

$$\begin{aligned} \dot{x}_m &= A_m x_m + B_m r \\ y_m &= C_m^T x_m \end{aligned} \tag{50}$$

Then, in order for the closed control system to follow the reference model, it must be:

$$A_c \to A_m \ , \ B_c \to B_m \tag{51}$$

Therefore, to deduce the adaptation mechanism, we follow the following steps:

Step 1: Deriving the error equation:

The error vector is given by the state variables in the following formula:

$$e = x_p - x_m \tag{52}$$

Whereas:

$x_p = \left[x_{p1}, x_{p2}, \ldots, x_{pn}\right]^T$ It is a vector of state variables for the control statement.

$x_m = [x_{m1}, x_{m2}, \ldots, x_{mn}]^T$ It is a vector of state variables for the reference model.

If the state equations for the closed loop control system are in the following form:

$$\dot{x}_p = A_c x_p + B_c r \tag{53}$$

The equations of state for the reference model are in the following form:

$$\dot{x}_m = A_m x_m + B_m r \tag{54}$$

By deriving the error equation (52):

$$\dot{e} = \dot{x}_p - \dot{x}_m \tag{55}$$

We substitute the error equation and find:

$$\dot{e} = A_c x_p + B_c r - A_m x_m - B_m r \tag{56}$$

By adding the two terms $A_m x_p - A_m x_p$ to equation (56), and some mathematical procedures, we obtain the error equation for the adaptive control system in its final form:

$$\dot{e} = A_m . e + A . x_p + B . r \tag{57}$$

Whereas:

$$A = A_c - A_m \ , \ B = B_c - B_m \tag{58}$$

We define the parameter error vector as the matrix ϕ, which includes the terms in A, B, and contains the regulator parameters $k_0, k_1, k_2, \ldots, k_n$, in the following general form:

$$\phi = \begin{bmatrix} b_{pn} k_0 - b_{mn} \\ -a_{p1} + b_{pn} k_1 + a_{m1} \\ . \\ . \\ . \\ -a_{pn} + b_{pn} k_n + a_{mn} \end{bmatrix}_{(n+m)\times 1} \tag{59}$$

Where the signal vector corresponding to the parameter error vector $\omega(t)$ has the following formula:

$$\omega(t) = \begin{bmatrix} r & x_{p1} & x_{p2} & \cdots & x_{pn} \end{bmatrix}^T_{(n+m)\times 1} \tag{60}$$

Therefore, the error equation can be written according to the following formula:

$$\dot{e} = A_m . e + b_I . \phi^T . \omega \tag{61}$$

Whereas:

$$\begin{aligned} & b_I = \begin{bmatrix} 0 & 0 & \ldots & 0 & 1 \end{bmatrix}^T, e(n\times 1), A_m(n\times n), e(n\times 1) \\ & b_I(n\times 1), \phi^T(1\times(n+m)), \omega(n+m)\times 1 \end{aligned} \tag{62}$$

Step 2: Assuming a Lyapunov function:
In order for the control output signal to follow the reference model signal, the error vector must end at the zero vector. To achieve this, we impose a Lyapunov function defined positively according to the quadratic formula as a function of the signal error vector $e(t)$ and the parameter error vector ϕ^T ‹, i.e. of the following general form:

$$V(e,\phi)=e^T.P.e+\phi^T.\Gamma^{-1}.\phi \qquad (63)$$

Since $\Gamma^{-1}=\Gamma>0$ is a positively defined symmetric matrix called the adaptive gain matrix, and $P^{-1}=P>0$ is a positively defined symmetric matrix. For tracking to be possible, the derivative of the time-dependent Lyapunov function must be negatively defined. By differentiating the Lyapunov function, we find:

$$\dot{V}(e,\phi)=\dot{e}^T.P.e+e^T.P.\dot{e}+\dot{\phi}^T.\Gamma^{-1}.\phi+\phi^T.\Gamma^{-1}.\dot{\phi} \qquad (64)$$

For $\dot{V}(e,\phi)$ to be a negative identifier, we assume:

$$A_m^T.P+P.A_m=-Q \qquad (65)$$

By following the mathematical procedures that ensure that the derivative of the Lyapunov function is defined as negative, we obtain the adaptation law in its final form:

$$\dot{\phi}=-\Gamma.e^T.P.b_I.\omega \qquad (66)$$

6.3 Vehicle Suspension System Responses When Using the Adaptive Controller:

By applying the adaptive control methodology described in paragraph (6-2) and for the uncertainty shown in Table (2), we obtain the following simulation results:

6.3.1 Adaptive Controller Design Results for Nominal Parameters

For the nominal values of vehicle suspension system parameters, we obtain the following responses:

- **Response to vehicle body displacement y_1:**

Figure (19) shows the response to vehicle body displacement y_1 (t) when using the adaptive controller with the reference model:

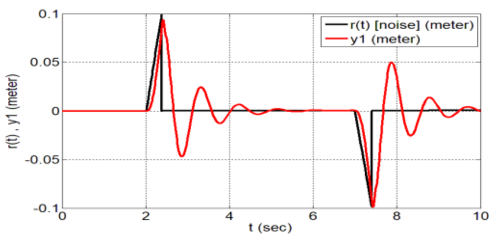

Figure 19 Response to vehicle body displacement y_1 when using the adaptive controller at the nominal values of the parameters

- **Response to the displacement of the cart wheels y_2**

Figure (20) shows the response to the displacement of the cart wheels $y_2(t)$ when using the adaptive controller:

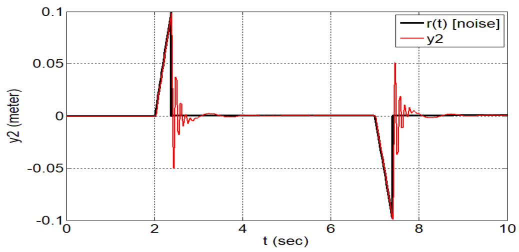

Figure 20 Response to vehicle wheel displacement $y_2(t)$ when using the adaptive controller at the nominal values of the parameters

6.3.2 Adaptive Controller Design Results with Parameter Uncertainty

For uncertainties in vehicle suspension parameters according to Table (2), we obtain the following responses:

- **Response to vehicle body displacement y_1**

Figure (21) shows the response to vehicle body displacement $y_1(t)$ when using the adaptive controller for maximum and minimum parameter uncertainties:

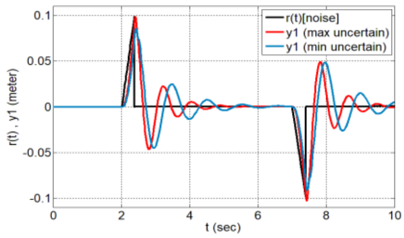

Figure 21 Response to vehicle body displacement $y_1(t)$ when using the adaptive controller for maximum and minimum uncertainty of parameters

- **Response to vehicle wheel displacement y_2:**

Figure (22) shows the response to vehicle wheel displacement $y_2(t)$ when using the adaptive controller for maximum and minimum uncertainty in the parameters:

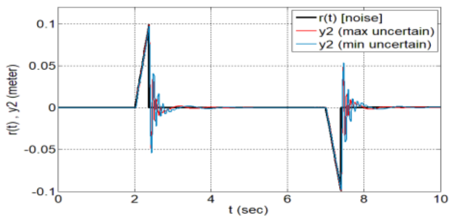

Figure 22 Response to vehicle wheel displacement $y_2(t)$ when using the adaptive controller for maximum and minimum uncertainty of parameters

From the previous responses, especially the vehicle displacement response $y_1(t)$ shown in Figure (19) and corresponding to the nominal values of the parameters, we note that the response is poor, as the maximum displacement of the vehicle body reached about (0.1 meter) for the maximum road deformation (0.1 meter) and the minimum (-0.1 meter). We note that the vibration damping required a time of about (2 seconds) for the vehicle level to return to a completely straight position. When the vehicle total parameters are uncertain due to the decline in the flexibility of the suspension system due to the temperature and surrounding climatic conditions, and according to Figure

(21), we note that for the maximum uncertainty, the displacement of the vehicle body reached (0.1 meter), and for the minimum uncertainty, the displacement of the vehicle body reached (0.08 meter). Thus, we conclude the success of the adaptive controller in absorbing the maximum and minimum road deformations, but with a large displacement of the vehicle body, which negatively affects the comfort of passengers.

According to Figures (20) and (22), which show the vehicle wheel displacement response $y_2(t)$, we note that the maximum displacement is 0.1 meters for the nominal parameter values and the maximum and minimum parameter uncertainties. Note that the vehicle body response is most important because it contains passengers whose comfort and calm are to be maintained during travel while exposed to various road deformations.

7. COMPARING THE RESULTS OF THE OPTIMAL PARAMETRIC CONTROLLER AND THE ADAPTIVE CONTROLLER

The responses of the optimal and adaptive parametric controllers will be compared for the nominal parameter values and for the maximum and minimum parameter uncertainties.

7.1 Comparison of the vehicle body displacement response y_1 when using the optimal and adaptive parametric controllers for the nominal parameters

Figure (23) shows the response to the vehicle body displacement $y_1(t)$ when using the optimal and adaptive parametric controllers with the reference model:

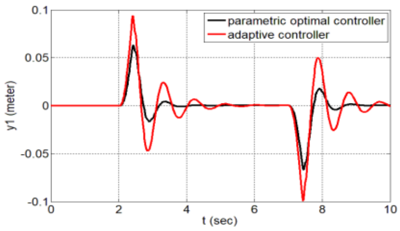

"Figure 23" Response to vehicle body displacement $y_1(t)$ when using the optimal and adaptive parametric controller at the nominal values of the parameters

7.2 Adaptive Controller Design Results with Parameter Uncertainty:

For uncertainties in vehicle suspension parameters according to Table (2), we obtain the following responses:

- **Response to vehicle body displacement $y_1(t)$ at maximum parameter uncertainty:**

Figure (24) shows the response to vehicle body displacement $y_1(t)$ when using the optimal and adaptive parametric controller for maximum parameter uncertainty:

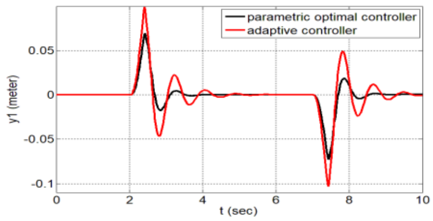

"Figure 24" Response to vehicle body displacement $y_1(t)$ when using the optimal and adaptive parametric controller for maximum uncertainty in the parameters

- **esponse to vehicle body displacement $y_1(t)$at minimum uncertainty in parameters:**

Figure (25) shows the response to vehicle body displacement $y_1(t)$when using the optimal and adaptive parametric controller for minimum uncertainty in parameters:

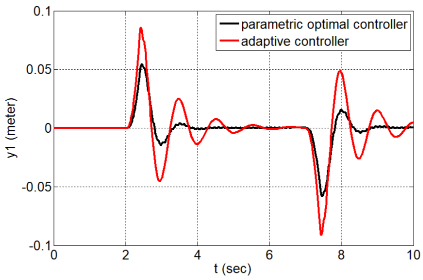

Figure 25 Response to vehicle body displacement $y_1(t)$ when using the optimal and adaptive parametric controller for minimum uncertainty in the parameters

From the previous responses, especially the response of the displacement of the vehicle $y_1(t)$ shown in Figure (23) corresponding to the nominal values of the parameters, and Figure (24) corresponding to the maximum uncertainty of the parameters, and Figure (25) corresponding to the minimum uncertainty of the parameters, we notice that the optimal parametric controller always outperforms the adaptive controller. This is because the design of the optimal parametric controller takes the uncertainty of the parameters into account in the design algorithm, while the adaptive controller needs to calibrate the adaptation gains when the parameters change, and this makes the matter difficult, because the adaptation gains are adjusted once.

8. SIMULATION AND RESULTS

From the simulation results of the vehicle suspension system, we note that both the optimal and adaptive parametric controllers with the MRAC reference model achieved stable vehicle body and wheel displacement for the nominal values of the vehicle suspension system parameters and when these parameters are uncertain within a range of $\pm 20\%$. The simulation results demonstrate the superiority of the optimal parametric controller over the adaptive controller. For the nominal values of the parameters, when using the optimal parametric controller, we note that the range of maximum and minimum vehicle body displacement is approximately $\pm 0.05\,meter$ for the maximum (0.1 meters) and minimum (-0.1 meters) road deformation. When using the adaptive controller, the range of vehicle body displacement is approximately $\pm 0.1\,meter$ for the maximum (0.1 meters) and minimum (-0.1 meters) road deformation. When the control system parameters are uncertain, the optimal parametric controller remains the best. Outperforming the adaptive controller.

9. REFERENCES

[1] Saeed Yaghoubi, Afshin Ghanbarzadeh,2024. "Modeling and optimization of car suspension system in the presence of magnetorheological damper using Simulink-PSO hybrid technique", Results in Engineering,journalhomepage: www.sciencedirect.com/journal/results-in-ngineering,.

[2] Ambarish Kulkarni, Sagheer A Ranjha, and Ajay Kapoor, 2017. "Aquarter-car suspension model for dynamic evaluations of an in-wheel electric vehicle", Journal of Autmobile Engineering.

[3] M Umais Shabbir, 2021. "Design and Analysis of Vehicle Suspension System", ReaserchGate.

[4] K.Dhananjay Rao, 2014. "Modeling, Simulation and Control of Semi Active Suspension System for Automobiles under MATLAB Simulink using PID Controller ", Third International Conference on Advances in Control and Optimization of Dynamical Systems March 13-15, 2014. Kanpur, India, IFAC,.

[5] Gaurav Chaudharya Manoj Kumarb, Santosh Vermac Anupam Srivastav,2014. “Optimization of drilling parameters of hybrid metal matrix composites using response surface methodology”, ScienceDirect, Procedia Materials Science 6 229 – 237, 3rd International Conference on Materials Processing and Characterisation (ICMPC 2014), 2014.

[6] Ammar Majid Hameed Al-Ghanim, Dr. Ameen Ahmed Nassar, 2016."Modeling, Simulation, and Control of Half Car Suspension System Using Matlab/Simulink", International Journal of Science and Research (IJSR) ISSN (Online): 2319-7064 Index Copernicus Value (2016): 79.57 | Impact Factor (2015): 6.391,

[7] Davor Hrovat, H. Eric Tseng and Joško Deur, 2019."Optimal Vehicle Suspensions: A System-Level Study of Potential Benefits and Limitations" , CISM International Centre for Mechanical Sciences P. Lugner (ed.), Vehicle Dynamics of Modern Passenger Cars, CISM International Centre for Mechanical Sciences 582, https://doi.org/10.1007/978-3-319-79008-4_3,

[8] Mauricio Sobrino y Arjona-Guzman and Moises Jimenez-Martinez*, Member, IAENG, and Sergio G. Torres-Cedillo 2022., “Vehicle Performance Assessment Using the OBD2 Port and Artificial Neural Network”, Engineering Letters, 30:4, EL_30_4_08, ResearchGate,

[9] Sayel M. Fayyad,2012. "Constructing Control System for Active Suspension System", Contemporary Engineering Sciences, Vol. 5, 2012, no. 4, 189 – 200,.

[10] Ajit G. Mohite, Anirban C. Mitra, 2017."Development of Linear and Non-linear Vehicle Suspension Model ", Available online at www.sciencedirect.com ScienceDirect Materials Today: Proceedings 5 (2018) 4317–4326, ICMPC,

[11] Hassan Ahmad Metered, 2010."Modelling and control of magnetorheo logical dampers for vehicle suspension systems”, school of mechanical, aerospace and civil engineering.

[12] walelign Wudu Bezabh,2023. "Quarter Car Suspension System Modelling, Simulation, And Performance Analysis under Dynamic Conditions", Research Square,

[13] Paul Oke, Jone Tawaketini, Niranjan Singh, 2023."Robust Control of Active Suspension System using MATLAB/Simulink", 979-8-3503-2971-1/23/$31.00 ©2023 IEEE,

[14] Sarthak Vaishnav, Jerry Paul, Deivanathan R, 2021."Model development and simulation of vehicle suspension system with magneto-rheological damper", IOP Conf. Series: Earth and Environmental Science 850 (2021) 012035,

[15] Roland S.Burns, 2001."Advanced Control Engineering", Buttrworth Heinemann, Adivision of reed eduvcational and professional publishing Ltd,

[16] Feng Lin, 2007." Robust Control Design An Optimal Control Approach", John Wiley & Sons Ltd, The Atrium, Southern Gate, Chichester, West Sussex PO19 8SQ, England Telephone +44 1243 779777,

[17] Matthew C. Turner Declan G. Bates, 2007."Mathematical Methods for Robust and Nonlinear Control", Lecture Notes in Control and Information Sciences, Springer,

[18] Shanker sastry, Marc bodson, 2000."ADAPTIVE CONTROL stability, convergence,and robustness", Perntice Hall Advanced Reference Series,

[19] Shengyang LI, 2013." Adaptive Multi-reservoir-based Flood Control and Management for the Yellow River ", CSC Press/Balkema is an imprint of the Taylor & Francis Group, an informa business © 2013, Shengyang LI,

[20] Hong SONG2011., "Model-based Control in Adaptive Optics Systems", Printed in The Netherlands Author’s email: cdreaming@gmail.com,

[21] Amir F. Ajami, 2005." Adaptive Flight Control in the Presence of Input Constraints ", Blacksburg, Virginia, December 2,

[22] Nhan T. Nguyen,, 2008. "Robust Optimal Adaptive Control Method with Large Adaptive Gain", American Institute of Aeronautics and Astronautics.

[23] Liviu Popescu,, 2010. " On control and systems", M.S.C.: 17B66, 93B05